SMAR 2017 – Fourth Conference on Smart Monitoring,
Assessment and Rehabilitation of Civil Structures

SMAR 2017

Modeling the bond of GFRP and concrete based on a damage evolution approach

Mohammadali Rezazadeh[1], Valter Carvelli[2], and Ana Veljkovic[3]

[1] Dep. Architecture, Built environment and Construction engineering, Politecnico di Milano, Italy
[2] Dep. Architecture, Built environment and Construction engineering, Politecnico di Milano, Italy
[3] Dep. Architecture, Built environment and Construction engineering, Politecnico di Milano, Italy

ABSTRACT: The effect of debonding of glass-fiber-reinforced-polymer (GFRP) reinforcing bar on progressive collapse resistance of concrete structures is an important point in the design of GFRP reinforced concrete structures. Due to the complexity of the GFRP-concrete debonding failure, numerical analyses are necessary to better understand the influence of several parameters on this failure mode. Hence, the current paper aims to develop a 3D finite-element (FE) model, capable of predicting the debonding failure by modeling the GFRP bar-concrete bond interface using cohesive elements. The damage assessment approach is adopted to determine the properties of the bond interface. Moreover, the model considers the nonlinear behavior of concrete. At the end, the good predictive performance of the developed FE model is demonstrated by comparing with the relevant experimental results.

1 INTRODUCTION

Corrosion-free fiber reinforced polymer (FRP) materials have been developed as an alternative to steel to reinforce the concrete elements due to the several advantages. Among the available FRP composite materials in the market, glass fiber reinforced polymer (GFRP) reinforcements have received considerable attention due to its cost competitive advantages (Yan et al. 2016). The efficiency of GFRP reinforcements in structural applications may be limited by the occurrence of GFRP-concrete debonding (ACI 440.1R 2015, Yan et al. 2016). The literature review shows that the anisotropy nature of GFRPs introduces more complexities to predict the GFRP-concrete bond characteristics compared to the steel-concrete counterpart. To reduce as much as possible the cost of experimental testing, the numerical analyses are necessary to evaluate the influence of several parameters on the bond behavior of GFRP bar and concrete (Fava et al. 2016, Yan and Lin 2016).

This study intends to develop a 3D finite element (FE) model to numerically simulate the GFRP-concrete bond behavior. The model considers the nonlinear behavior of concrete and the GFRP bar-concrete interface based on a damage evolution approach, using a commercial FE software. The good predictive performance of the developed FE model is demonstrated by simulating and comparing with the results of the relevant experimental eccentric pullout tests. At the end, the influence on the bond behavior of the key parameter in the used damage approach was numerically investigated.

2 THEORETICAL BACKGROUD OF THE NUMERICAL MODEL

The main objective of the present section is to theoretically explain the developed finite element (FE) model to simulate the bond behavior between the GFRP bar and concrete. The nonlinearity in GFRP bond behavior was simulated by adopting a bond damage evolution approach. The damage approach consists of two requirements: a damage initiation criterion (2nd step in Figure 1a) and a damage evolution law (3rd step in Figure 1a). The maximum bond shear stress derived from the known bond shear stress-slip curve can be defined as a damage initiation criterion. Once the damage initiation criterion occurs, the damage propagation follows the adopted damage evolution law. The damage evolution law in this study is assumed to have an exponential softening branch (3rd step in Figure 1a), which is calibrated by curve fitting of the known bond shear stress-slip curve. Regarding the pre-peak state of bond behavior, an initial linear response is assumed up to the maximum bond shear stress (τ_b) (1st step in Figure 1a).

The exponential softening law of bond shear stress-slip relation defines the bond damage variable (D) as a function of the slip (δ) beyond the damage initiation. The bond damage variable (D) ranges between 0 (denoting no damage) and 1 (denoting the limit state of damage) (Figure 1b). This bond damage variable (D), expressed in Eqn. (1), is specified by a non-dimensional parameter (α), the slips corresponding to maximum bond stress (δ_b) and to complete failure (δ_u , see Figure 1a) (ABAQUS 2013). The α parameter in Eqn. (1) is determined from the curve fitting of the known bond shear stress-slip curve.

$$D = \begin{cases} 0, & \delta \le \delta_b \\ 1-\left(\dfrac{\delta_b}{\delta}\right)\left(1-\dfrac{1-\exp\left(-\alpha\left(\dfrac{\delta-\delta_b}{\delta_u-\delta_b}\right)\right)}{1-\exp(-\alpha)}\right), & \delta > \delta_b \end{cases} \tag{1}$$

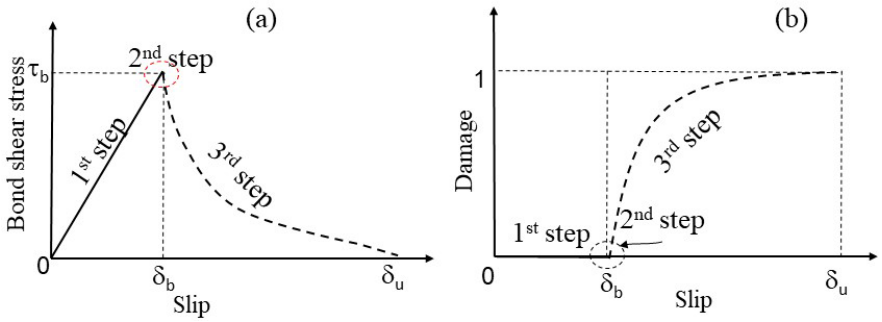

Figure 1. a) Bond shear stress-slip relation with exponential softening branch, b) Bond damage parameter *D* vs. slip.

The bond behavior of the GFRP bar-concrete interface was simulated using cohesive elements by defining the relevant bond properties. The latter was built based on the mentioned exponential bond-slip law (Figure 1), and assigned to the cohesive element with a thickness close to zero

(0.001 mm). Both main surfaces of cohesive element layer are tied to the surrounding components using a surface-based tie constraint (no-slip occurrence). A mixed mode of bond behavior including stress-separation (in the normal direction of the cohesive element plane) and shear stress-slip (on both tangential directions of the cohesive element plane) was used to simulate the GFRP bar-concrete bond.

The initial elastic bond shear stiffness (K_s) is defined as the ratio between τ_b and δ_b ($K_s = \tau_b / \delta_b$) deriving from the known bond shear stress-slip relation. Moreover, the GFRP bar-concrete bond normal response was assumed to be linear in this analysis considering the proposal of effective bond normal stiffness (K_n), as follows:

$$K_n = \frac{K_{nf} . K_{nc}}{K_{nf} + K_{nc}} \tag{2}$$

where $K_{nf} = E_{nf} / t_{nf}$ is the stiffness of GFRP bar in normal direction (E_{nf} and t_{nf} are, respectively, the modulus of elasticity of GFRP bar in the direction normal to its longitudinal axis and the thickness of GFRP bar which is expressed by $t_{nf} = \phi / 2$, ϕ is the bar diameter). $K_{nc} = E_c / t_{nc}$ is the stiffness of concrete surrounding the GFRP bar in normal direction (E_c is the modulus of elasticity of concrete, and t_{nc} is a thin layer of concrete that is influenced by the normal stress exerting by the GFRP). By inspiring on the works of (Dai et al. 2005, Rezazadeh and Barros 2015), t_{nc} was assumed to be 45 mm or cover thickness in simulations.

For modeling the nonlinearity in concrete, the concrete damage plasticity (CDP) model was used in the numerical analysis. The constitutive parameters of the CDP model includes: dilation angle $\psi = 38^{\circ}$, plastic potential eccentricity $e = 0.1$, stress ratio $f_{bo} / f_{co} = 1.16$ (ratio between the compressive strength in bi- and uniaxial compression, f_{bo} and f_{co}, respectively), shape of the loading surface $K_c = 0.67$, and viscosity parameter $V = 0$ (Kmiecik and Kamiński 2011, ABAQUS 2013). The uniaxial behavior for the uncracked concrete was assumed to be linear up to f_{ct} (concrete tensile strength) and $0.45 f_c$ (concrete compressive strength) (Rezazadeh et al. 2016). For the cracked concrete, the uniaxial behavior is derived from the recommendations of CEB-FIP (2010) model code using a stress-crack opening and stress-strain relations in tension and compression zones, respectively (CEB-FIP 2010).

GFRP bar was assumed to behave linearly elastic up to its ultimate tensile strength without any plastic deformation. Accordingly, a transversely isotropic linear elastic material model was used to characterize the GFRP bars considering the properties declared in producer's catalogue and the prediction of the mechanical properties by the rule of mixture and Chamis's formulae (Chamis 1989).

3 MATERIALS AND SOME EXPERIMENTAL FEATURES

The experimental program (Veljkovic et al. 2017), here summarized, was considered for assessing the predictive performance of the developed FE model. This experimental program was comprised of quasi-static pullout tests to access the bond characteristics between GFRP bar and concrete. In the present pullout tests, one bar type and diameter (ComBAR® GFRP bar, $\phi 8$ mm, with ribbed surface, Figure 2a) was selected in combination with 3 different concrete mixtures (S1, S2, and S3, Table 1) and 2 different eccentric positions of the bar inside the concrete

specimen (concrete cover of 10 and 20 mm, Table 2). Mechanical properties in the bar (fibers) direction are assumed, according to producer's catalogue, as follows: tensile strength of 1500 MPa and modulus of elasticity of 60 GPa.

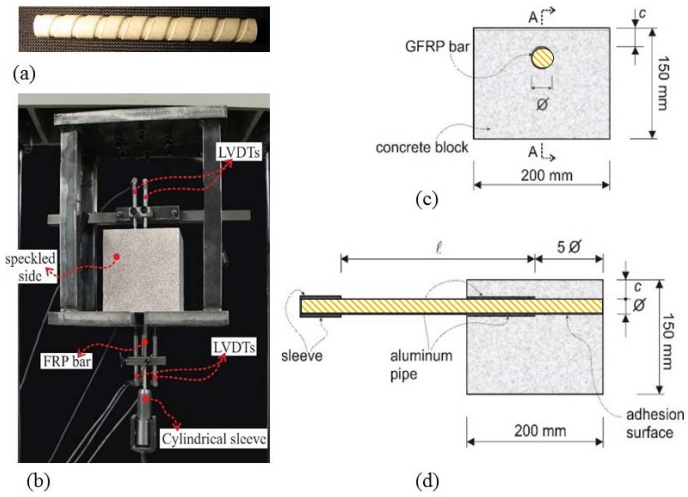

Figure 2. a) Surface of the GFRP rebar ComBAR, Ø8mm, b) experimental setup, Pullout specimen geometry: (c) top view, (d) longitudinal section A-A.

Table 1. Mechanical characteristics of the considered concretes

Concrete ID	Compressive strength f_c^{cube} (MPa)	Tensile strength f_{ct} (MPa)	Modulus of elasticity E_c (MPa)
S1	23.3	2.29	19.71
S2	38.9	3.32	22.45
S3	56.3	3.96	27.88

Table 2. Overview of performed tests and specimen ID

Concrete ID	Concrete cover (mm)	Specimen ID
S1	10, 20	S1C10, S1C20
S2	10, 20	S2C10, S2C20
S3	10, 20	S3C10, S3C20

Embedment length of the bar was selected as 5ϕ (40 mm) and it was the same for all specimens (Figures 2c and 2d). Along the remaining part of the bar, an aluminum pipe was inserted to prevent bond between bar and concrete. Quasi-static pullout tests were performed by the test setup shown in Figure 2b. Crosshead displacement rate was set to 1 mm/min.

The bond damage curves of the experimental pullout tests were determined using the damage model previously introduced. In Figure 3, the bond damage parameter evolution vs. normalized slip relations of all the specimens are compared. The normalized slip is the slip of the pullout response divided by the corresponding δ_b of the specimen. By analyzing the damage parameter evolution curves, a critical bond damage level can be associated with the portion having the highest slope variation in the post-peak phase (see in Figure 3). This level corresponds to the force range in the transition of bond mechanism based on mechanical interlock and on residual friction between the bar and concrete. For the pullout tests analyzed in the present study, the critical bond damage level is estimated in the shaded area of Figure 3. The values determined for the parameters of the exponential model considering the experimental bond shear stress-slip curves are summarized in Table 3.

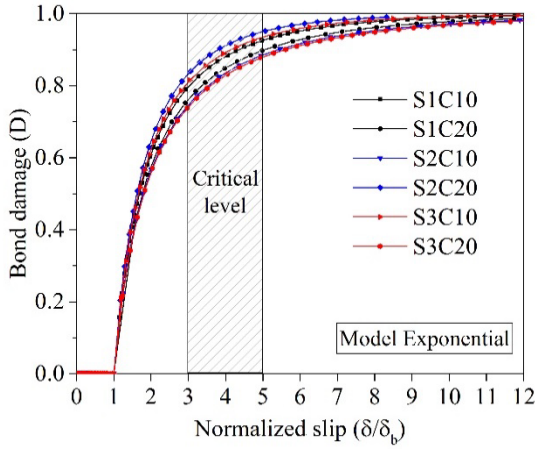

Figure 3. Comparison of the bond damage parameter evolution of the pullout tests.

Table 3: Relevant characteristics of bond for the damage model derived from the experimental data

Specimen	τ_b (MPa)	δ_b (mm)	δ_u (mm)	K_e ($N/mm^2/mm$)	α
S1C10	8.49	0.56	20	15.16	8.56
S1C20	7.90	0.59	20	13.39	5.51
S2C10	9.61	0.47	20	20.45	5.85
S2C20	8.23	1.07	20	7.69	6.14
S3C10	12.01	0.63	20	19.06	8.70
S3C20	12.80	0.61	20	20.98	3.91

4 NUMERICAL PREDICTIONS AND COMPARISONS

To assess the performance of the developed FE model, the described experimental pullout tests were numerically simulated by taking the advantage of one symmetry plane of the tests to reduce the computational time of analysis (see Figure 4). Accordingly, the boundary condition corresponding to the symmetry plane was applied to the FE models. Moreover, the support and loading conditions were simulated according to the characteristics of the test setup in the laboratory (see Figures 2 and 4). Eight-node 3D solid hexahedral elements (C3D8R element) were used to model the concrete and GFRP bars, while eight-node 3D cohesive elements (COH3D8 element) were adopted to model the bond zone.

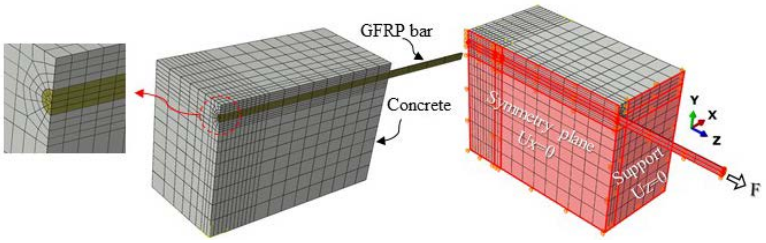

Figure 4. Geometry, boundary and loading conditions of the FE model.

As noted, the exponential softening branch was used for the bond damage modeling. The values of α parameter for the exponential damage model were adopted same as the ones reported in Table 3. The bond shear stress vs. slip responses registered experimentally and obtained numerically are compared in Figure 5. This figure evidences that all the bond responses, predicted by the adopted damage evaluation law, matched well with the experimental pullout test results, yielding a good accuracy and predictive performance for the FE model.

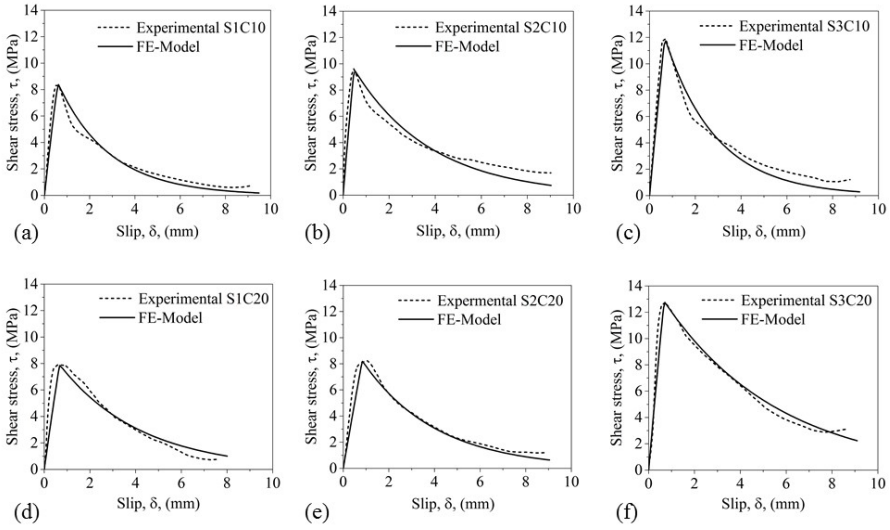

Figure 5. Comparison between the experimental and numerical bond behavior of the pullout specimens

5 CONTROL PARAMETER OF DAMAGE EVOLUTION RATE

The main objective of this section is to numerically evaluate the influence of α parameter, expressed in Eqn. (3), on the bond shear stress-slip relation and damage evolution curve, using the described FE model. The S1C10 pullout specimen was used for the present numerical evaluation. For the comparison purpose, the α parameter values of 0.001, 4, 16, and 32 were numerically adopted, which are almost 0, 0.5, 2, and 4 times the α parameter value adopted in the FE model of S1C10 specimen (8.56) derived from the experimental curve fitting (see Table 3). It should be noted that a value close to zero (0.001) was adopted for the α parameter, since it cannot be zero according to the Eqn. (1).

Figure 6a shows the bond-slip relations of the S1C10 FE model derived by adopting different values for the α parameter. This figure evidences that the α parameter is accountable to control the rate of damage evolution beyond the damage initiation. In other words, by increasing the α parameter, the bond damage in post-peak phase produces more rapidly, while adopting a value close to zero for α parameter, yields an almost linear bond softening branch. These effects of α can be confirmed by considering the damage evolution curves represented in Figure 6b derived numerically using the exponential damage model.

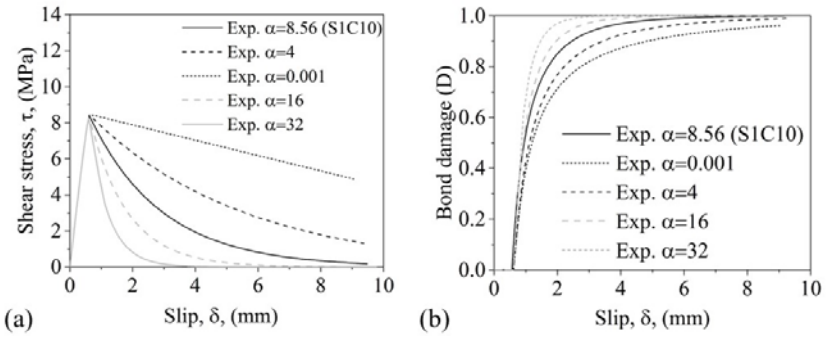

Figure 6. Influence of control parameter of damage evolution rate on: a) bond shear stress-slip relation, b) damage parameter D evolution

By increasing the concrete cover, a higher confinement to the GFRP bar is provided by the surrounding concrete. This higher confinement, in addition of delaying the concrete splitting failure, may provide higher resistance to slip development, resulting in a lower damage evolution rate. This fact can be confirmed from the experimental point of view by considering the reported α parameter in Table 3, where the pullout specimens of S1 and S3 (S1C10, S1C20, S3C10, and S3C20) showed a lower α for higher concrete cover thickness. However, the S2C10 and S2C20 specimens showed an almost similar value for α by increasing the concrete cover thickness.

6 CONCLUSIONS

The current work has developed a 3D nonlinear finite element (FE) model for simulating the behavior of GFRP bar-concrete bond. The FE model is capable of considering the nonlinear behavior of concrete and the GFRP bar-concrete bond interface. A bond damage approach based on an exponential softening branch was presented and used to simulate the GFRP bar-concrete interface properties. This damage approach depends on α parameter deriving from the curve fitting of experimental data. The developed FE model was used to simulate the experimental results of eccentric pullout tests. The good predictive performance of the FE model in terms of

the bond shear stress-slip relation was demonstrated. From the numerical parametric studies, it was verified that the α parameter is accountable to control the rate of damage evolution beyond the damage initiation. By increasing the concrete cover, due to the higher confinement provided to the GFRP bar by the surrounding concrete, a lower damage evolution rate is expected to occur. Considering the outcomes of this study, the numerical model presented here can give a contribution to increase the confidence in adopting such GFRP reinforcement in concrete structural elements.

7 ACKNOWLEDGMENTS

The research was developed in the framework of the Marie Curie Initial Training Networks – "endure" European Network for Durable Reinforcement and Rehabilitation Solutions, project no: 607851. Schöck Bauteile GmbH is gratefully acknowledged for supplying the GFRP rebars.

8 REFERENCES

ACI 440.1R, 2015, Guide for the design and construction of structural concrete reinforced with FRP bars, *ACI Committee 440*.

ABAQUS, 2013, Abaqus 6.14–Analysis Users's Guide: Volume IV: Elements, *Systèmes, Dassault*.

CEB-FIP, 2010, Model Code 2010. Final draft. *The International Federation for Structural Concrete*, Lausanne, Switzerland.

Chamis, C., 1989, Mechanics of composite materials: past, present, and future, *Journal of Composites, Technology and Research* 11(1): 3-14.

Dai, J., T. Ueda, and Y. Sato, 2005, Development of the nonlinear bond stress–slip model of fiber reinforced plastics sheet–concrete interfaces with a simple method. *Journal of Composites for Construction* 9(1): 52-62.

Fava, G., V. Carvelli, and M. Pisani, 2016, Remarks on bond of GFRP rebars and concrete. *Composites Part B: Engineering*, 93: 210-220.

Kmiecik, P. and M. Kamiński (2011). "Modelling of reinforced concrete structures and composite structures with concrete strength degradation taken into consideration." Archives of civil and mechanical engineering, 11(3): 623-636.

Rezazadeh, M. and J. Barros, 2015, Transfer zone of prestressed CFRP reinforcement applied according to NSM technique for strengthening of RC structures, *Composites Part B: Engineering*, 79: 581-594.

Rezazadeh, M., S. Cholostiakow, R. Kotynia and J. Barros, 2016, Exploring new NSM reinforcements for the flexural strengthening of RC beams: Experimental and numerical research, *Composite Structures*, 141: 132-145.

Veljkovic, A., V. Carvelli, M. Haffke and M. Pahn, 2017, Concrete cover effect on the bond of GFRP bar and concrete under static loading, *Composites Part B: Engineering*, Under Revision.

Yan, F. and Z. Lin, 2016, Bond behavior of GFRP bar-concrete interface: damage evolution assessment and FE simulation implementations, *Composite Structures*, 155: 63-76.

Yan, F., Z. Lin and M. Yang, 2016, Bond mechanism and bond strength of GFRP bars to concrete: a review, *Composites Part B: Engineering*, 98: 56-69.